

## Determination of Bentonite's Flow Limit Using Cylinder Strength Test and Suspension Settling Model

Samuel Jemmy Setiadjie<sup>1</sup>, Budijanto Widjaja<sup>2\*</sup>, Mayolus Musa Putra<sup>3</sup>,  
Atharayhan Anandito<sup>4</sup>

<sup>1</sup>Center for Geo-Hazard, Parahyangan Catholic University, Bandung, Indonesia, 40141; [samuel.setiadjie@unpar.ac.id](mailto:samuel.setiadjie@unpar.ac.id)

<sup>2</sup>Center for Geo-Hazard, Parahyangan Catholic University, Bandung, Indonesia, 40141; [widjaja@unpar.ac.id](mailto:widjaja@unpar.ac.id)

<sup>3</sup>Department of Civil Engineering, Faculty of Engineering, Parahyangan Catholic University, Bandung, Indonesia, 40141; [6102001024@student.unpar.ac.id](mailto:6102001024@student.unpar.ac.id)

<sup>4</sup>Department of Civil Engineering, Faculty of Engineering, Parahyangan Catholic University, Bandung, Indonesia, 40141; [alle.atharayhan@gmail.com](mailto:alle.atharayhan@gmail.com)

\*Correspondence: [widjaja@unpar.ac.id](mailto:widjaja@unpar.ac.id)

SUBMITTED 17 November 2025 REVISED 2 December 2025 ACCEPTED 6 December 2025

**ABSTRACT** Cohesive soils exhibit complex behavior characterized by distinct transitional boundaries between different states. One of the boundaries is the flow limit (FL), which is the transition between the viscous liquid and suspension states. Currently, there are no specific standard tests to determine the flow limit. Most previous studies have used the undrained shear strength ( $c_u$ ) value to determine the FL value. This study employed two different approaches to obtain the FL value: first, using the cylinder strength test (CST), which approaches from the viscous state, and second, using the suspension settling model, which approaches from the suspension state. There are five variations of samples for each test: 100% bentonite, 90% bentonite and 10% sand, 80% bentonite and 20% sand, 70% bentonite and 30% sand, and 60% bentonite and 40% sand. The cylinder tests were conducted with three different cylinder diameters: 30 mm, 40 mm, and 50 mm. For the suspension settling model, five solid concentrations were used, namely 5%, 4%, 3%, 2%, and 1%, for each sample. The results show that the CST for bentonite suspension gave higher FL values than the suspension settling model and CST; meanwhile, the suspension settling model is more conservative. The FL value from the CST test ranges from 3.33 to 4.9 times higher than the liquid limit (LL); the suspension settling model yielded values of 1.9 to 2.6 times higher than LL. The results are higher than those in previous studies (1.5 to 2 times higher than LL), which can be attributed to differences in apparatus capacities used to determine the  $c_u$  value, variations in bentonite mineral compositions, and different estimation approaches. In this study, the CST yielded more reliable FL values than the suspension settling model, which still entails numerous subjective assumptions.

**KEYWORDS** Cylinder Strength Test, Flow Limit, Suspension Settling Model, Suspension State, Viscous Liquid State

### 1 INTRODUCTION

Cohesive soils have several virtual boundaries that indicate the transitions between states. The state can be divided into solid state, semi-solid state, plastic state, viscous liquid state, and suspension state. Slurry materials are composed of cohesive soils between the viscous liquid and suspension states. Gary *et al.* (1977) stated that the suspension state occurs when soil particles are dispersed or separated from water particles. However, in the viscous liquid state, the soil and water particles are usually in a single phase or blended into a single material.

Atterberg (1911) proposed six limits, namely the upper limit of viscous flow (flow limit), liquid limit (LL), sticky limit, cohesion limit, plastic limit (PL), and shrinkage limit (SL), but most people are familiar with only the shrinkage limit, plastic limit, and liquid limit. The SL shows the transition point between the solid state and semi-solid state, PL is between the semi-solid state and the plastic state, and LL is between the plastic state and the viscous liquid state. However, there is no clear limit that separates the suspension state from the viscous liquid state for slurry materials.

Casagrande (1932), Germaine and Germaine (2009), and Park and Nong (2013) proposed a new limit that separates the suspension state from the viscous liquid state, known as the flow limit. The flow limit is not yet considered an international standard due to a lack of research, and there is no standardized test to define it. However, understanding the flow limit is essential to comprehending the soil behavior during the transition from a viscous liquid state to a suspension state. This condition can be observed during the hydrometer test (O'Brien, 2003).

This study aims to determine the FL value using two different approaches. The first is the Cylinder Strength Test (CST), which estimates FL from the viscous liquid side. The second is the suspension settling model, which approaches FL from the suspension side. This study focused on bentonite samples due to their exceptionally high water absorption capacity, which enables better suspension (Bain, 2009). This study involved five gradation variations of sand, combined with four additional variations of solid concentration for the suspension settling model, and three different cylinder diameters. This study aims to estimate the FL value using various approaches to determine the intersection range, thereby providing a more accurate understanding and a more reliable test for determining the value of FL.

## 2 LITERATURE REVIEW

### 2.1 Flow Limit (FL)

According to Germain and Germain (2009), the FL is the boundary between fluid and suspension states, where in the suspension state, solid and fluid particles have no contact forces, resulting in no effective stress within the material. Park and Nong (2013) define the FL as the point at which the undrained shear strength ( $c_u$ ) reaches a value of zero in between viscous liquid and suspension states. Typically, the flow limit is 1.5 to 2 times higher than the liquid limit value. Shen and Tsai (2024) offer an alternative perspective for flow landslide cases, defining FL as the moisture content at which the soil starts to flow at a certain inclination angles (32°-80°).

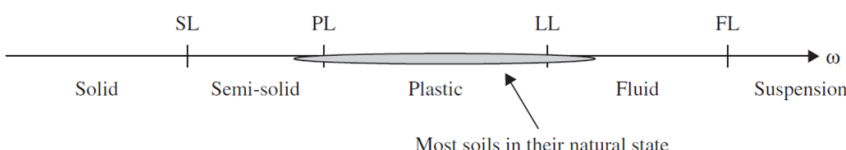


Figure 1. Flow limit and other Atterberg's Limits (Germain & Germain, 2009)

Some previous studies have employed various methods to determine the FL. Park and Nong (2013) used torvane (portable vane shear) to determine the  $c_u$  values at different water contents. They then extrapolated the  $c_u$  and water content curve to obtain the water content (FL) when the  $c_u$  value equals zero. Park and Nong (2013) show that FL is around 1.5 to 2.21 times higher than the LL. Widjaja and Florentini (2020) used the Fall Cone Penetrometer Test to determine the FL value, employing both the standard cone and a modified cone with a 4 g weight to obtain the  $c_u$  values, and extrapolated the result to reach the value of zero. It was found that FL is 1.5 to 1.6 times higher than the liquid limit. Shen and Tsai (2024) used the Atterberg liquid limit and flow limit instrument; they found that the FL is dependent on the slope angle for flow landslide cases, and the FL values are around 1.5 to 2 times higher than the LL values.

### 2.2 Cylinder Strength Test (CST)

Slurry material is a very weak material that sags under its own weight. Therefore, slurry samples cannot be tested with conventional shear strength tests, including vane shear or torvane, as they cannot measure very low undrained shear strengths ( $c_u$ ). Vallejo and Scovazzo (2003) proposed a new test, based on Sokolovski's theory (1995), using a cylinder, that calculates the indentation pressures developed by Tresca plastic when the cylinder penetrates it. This method involves slowly lowering a cylinder of known dimensions and weight into a mud sample under gravity. The cylinder diameter was 3.48 cm and the length is 7 cm. From the penetration depth, the  $c_u$  value can be

calculated using the bearing capacity principle and the buoyancy effect, as shown in Figure 2. Equations 1 and 2 show how to calculate the  $c_u$  value.

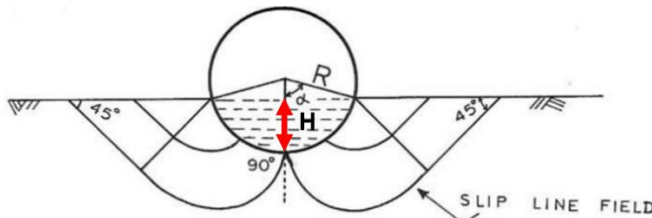


Figure 2. Cylinder strength test principle (after Vallejo, 2019)

$$c_u = \frac{R [\pi \gamma_c - (\alpha - \sin \alpha \cos \alpha) \gamma_f]}{2 [(\pi + 2) \sin \alpha + 2(1 - \cos \alpha - \alpha \sin \alpha)]} \quad (1)$$

$$\alpha = \cos^{-1} \left( \frac{R - h}{R} \right) \quad (2)$$

where  $R$  is the radius of the cylinder,  $\gamma_c$  is the cylinder unit weight,  $\gamma_f$  is the mud unit weight, and  $h$  is the immersed cylinder height.

### 2.3 Suspension Settling Model

The suspension settling model is a model that helps us understand the sedimentation process of soil particles, which has been used since the Stone Age (Concha, 2014). This test utilized the extension of Stokes' equation and other empirical modelling (Egolf & McCabe, 1937). Mishler (1912) and Coe and Clevenger (1916) recognized that the settling of a homogeneous flocculent suspension has four settling zones. The four settling zones, namely clear water (zone A), initial concentration (zone B), transition zone (zone C), and compression zone (zone D), are illustrated in Figure 3.

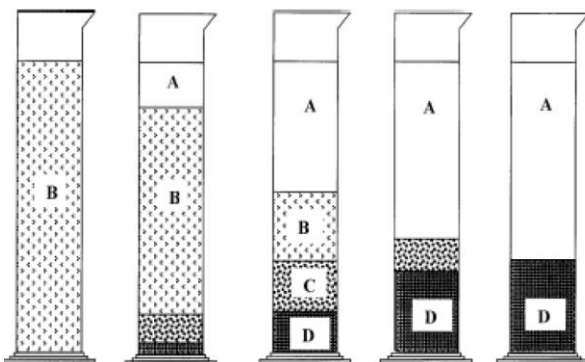


Figure 3. Suspension Settling Model (after Coe & Clevenger, 1916)

Figure 4 shows the settling cycle of a suspension based on Kynch's (1952) theory, where the sedimentation velocity only depends on particle concentrations. There are mudlines and sludge lines, where the mudline indicates where the suspension behaves like mud, and the sludge line marks the boundary between suspension and sedimentation. The critical sedimentation velocity ( $v_c$ ) can be calculated using Equation 3, where  $v_c$  is determined by the completion of sedimentation and indicates the limit at which the sample has reached equilibrium (the separation is only Zone A and D), corresponding to the viscous liquid state limit.

The conclusion of the sedimentation process is recognized when the sedimentation velocity diminishes below a specified critical threshold, as denoted by an exceedingly low  $v_c$ , thereby indicating the completion of the process (Kynch, 1952). Essential parameters, including the critical suspension height ( $H_c$ ) and critical time ( $t_c$ ), delineate the transition to a viscous liquid state as well as the point at which the sediment achieves full compression at the base. To verify the viscous liquid

condition at the base of the sample, assessments such as water content and index properties are undertaken, encompassing the LI and FL, which demonstrate that the soil maintains shear strength despite its viscous state.

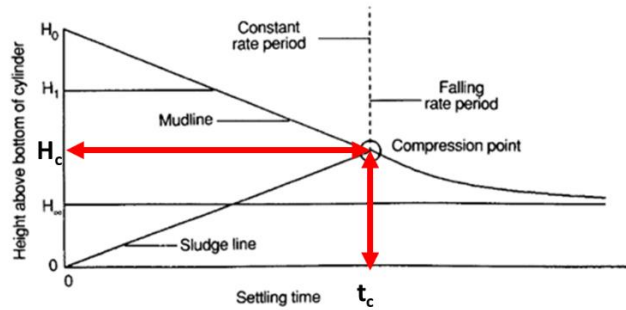


Figure 4. Settling cycle of a suspension (El-Shall *et al.*, 1993)

$$v_c = \left( \frac{H_1 - H_c}{t_c} \right) \quad (3)$$

where  $H_1$  is the constant suspension height,  $H_c$  is the critical suspension height, and  $t_c$  is the critical time.

Conca (2014) states that the phase before the critical condition still undergoes the sedimentation process, where each particle has no force to interact with other particles. However, when the condition after the sample passes through the critical point, the sample is undergoing compression. In this case, compression means that the sample can interact with each other but cannot hold its weight and starts to be compressed; in other words, this condition indicates that the sample already has an effective stress.

Zhang *et al.* (2025) found that, during the compression phase, the van der Waals force was the first to dominate the particles' interaction. In the next phase, the particles undergo a densification process dominated by double-layer interaction. In the rarefaction phase, the yield stress is the dominant force to govern the interactions (Figure 5). Wesley (2009) gave a similar opinion. However, with a different perspective, where the deposition process (compression) stage is the first stage, where the stress of the soil is neglected, due to the high void and very soft consistency, while the soil volume is increasing at deposition area the stress will increase and start to compress itself by its own weight thus increasing the strength and reduces the void (Figure 6).

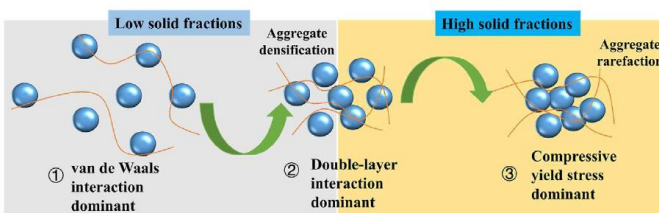


Figure 5. Illustration of particle interaction with the dominating force for each phase (Zhang *et al.*, 2025)

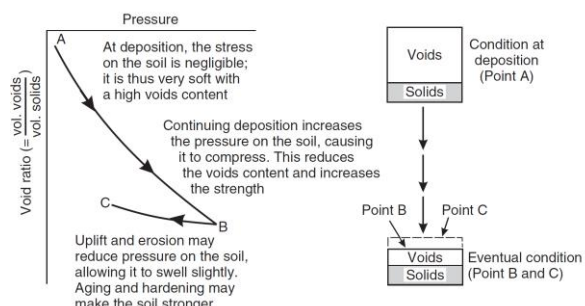


Figure 6. Sedimentary soils formation (Wesley, 2009)

### 3 METHODS

This study was done with five gradation variations of sand mixing (100% bentonite, 90% bentonite and 10% sand, 80% bentonite and 20% sand, 70% bentonite and 30% sand, and 60% bentonite and 40% sand). In the suspension settling model, there are four additional variations of solid concentration (solid to water ratio): 5% (50 g soil), 4% (40 g soil), 3% (30 g soil), and 2% (20 g soil). For the CST test, three cylinder diameters were used: 30 mm, 40 mm, and 50 mm. In this study, water content is presented as the liquidity index (LI) to normalize the water content values, accounting for sample variations.

The CST was conducted in an aquarium filled with a bentonite mixture using an acrylic cylinder. The bentonite mixture mixed the bentonite and water with a mixer until it is homogeneous (Figure 7a), and then placing the bentonite into the aquarium. The acrylic cylinder was placed on the mud and allowed to sink under its own weight until it came to rest (Figure 7b). The depth of the submerged part of the cylinder was then measured. The CST is performed at LI 1.4 (when the acrylic cylinder first penetrates to the mixture for this case), and then increases the water content until the cylinder is fully submerged. The increase in water content is calculated by determining the water needed for a specific LI value that starts from 1.4 to 2.9. To measure the submerged height, the cylinder was first picked up from the aquarium and then the height covered by the bentonite was measured using a caliper (Figure 7c).

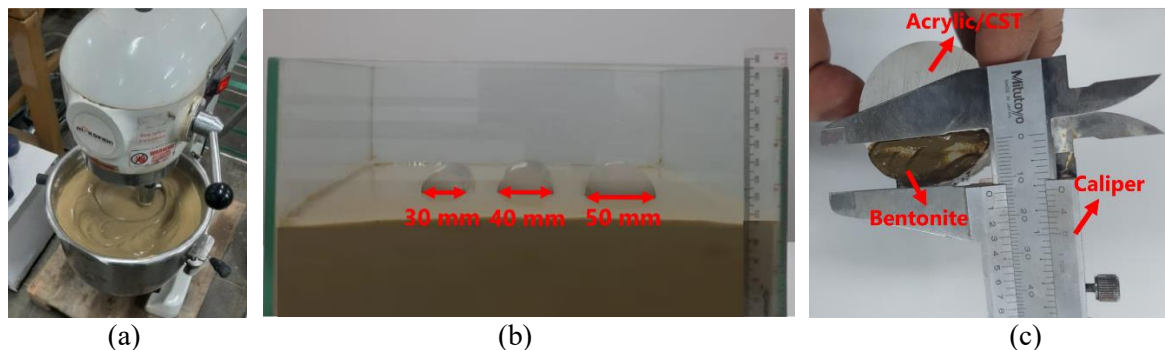


Figure 7. (a) Sample preparation; (b) CST illustration for 30 mm, 40 mm, and 50 mm diameters; (c) cylinder submerged height measurement using caliper.

For the suspension settling model, which utilized approximately 1000 ml sedimentation cylinders, the bentonite sample was mixed with 20 ml of dispersing agent (water glass), dissolved in 80 ml of water, and then mixed using a mixer until it became homogeneous. Next, the slurry is transferred to the sedimentation cylinders and diluted with water until a total volume of 1000 ml is reached. After that, the slurry is mixed by an agitator for 1 minute. During the initial phase, the slurry is observed at 1-minute intervals as it settles. When the sediment height increases by around 20 ml reading, the observation is conducted, and the test is stopped after five days. The illustration of the suspension settling model is shown in Figure 8.

After performing the suspension settling model test, the aqueous phase that separates from the bentonite sediment is removed. To validate the results, a CST was performed on the bentonite sediment using a 6 mm diameter and 40 mm long plexiglass cylinder. A metal clamp was used to drop the cylinder onto the sediment, and the submerged part was measured to obtain the  $c_u$  value. Figure 9 shows the CST process.

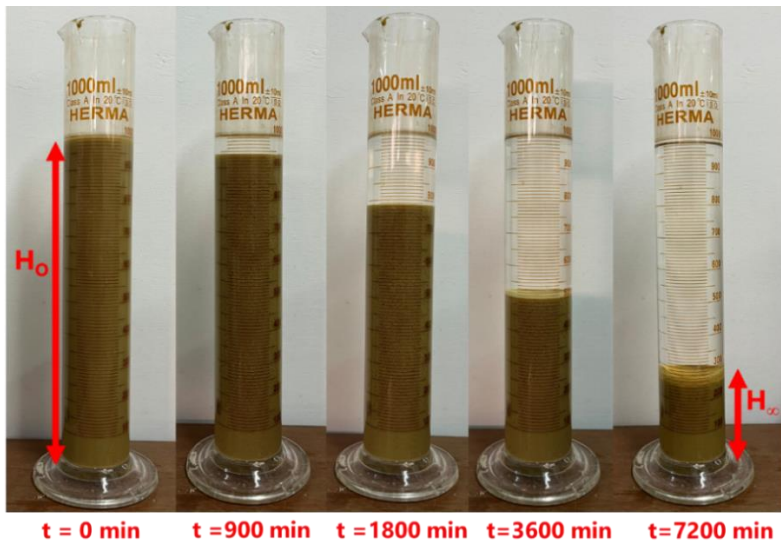


Figure 8. Suspension settling model simulation for bentonite sample

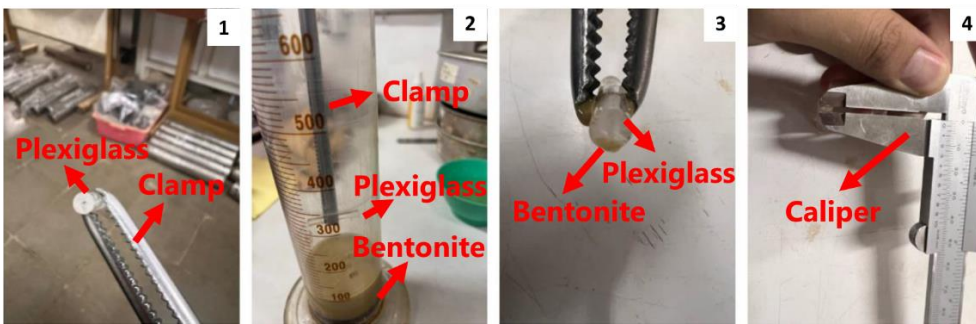


Figure 9. CST for the bentonite suspension sediment process

## 4 RESULTS AND DISCUSSION

### 4.1 Samples Index Properties

Before all the aforementioned tests were conducted, index properties tests were conducted on all specimens. The tests include the liquid limit (LL) and plastic limit (PL) tests using the fall cone penetrometer test, and specific gravity test. The results are shown in Table 1, it is evident that as the sand percentage increases, the LL and PL values decrease, while the  $G_s$  value increases. The grain size distributions of the specimens are shown in Figure 10. The results show that all bentonite variations are dominated by clay (more than 50%). Different than the % clay fraction, the behavior as indicated by Casagrande's plasticity chart (Figure 11) classifies all samples as MH (silt with high plasticity). The sand used in this study is dominated by medium sand (Figure 10) with a  $G_s$  value of 2.68.

Table 1. Index properties of all specimens

Paramters	Bentonite 100%	Bentonite 90% + Sand 10%	Bentonite 80% + Sand 20%	Bentonite 70% + Sand 20%	Bentonite 60% + Sand 40%
Liquid Limit (LL)	430	320	300	260	210
Plastic Limit (PL)	148	125	110	100	70
Specific Gravity ( $G_s$ )	2.67	2.68	2.69	2.73	2.76
Plasticity Index (PI)	282	195	190	160	140
Soil Classification	MH	MH	MH	MH	MH

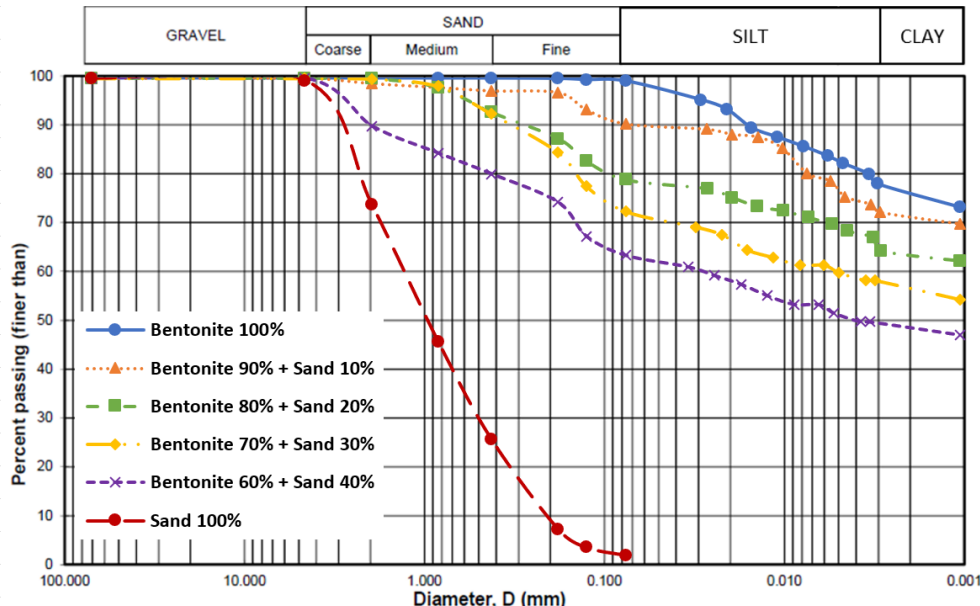


Figure 10. Grain size distribution of all specimens

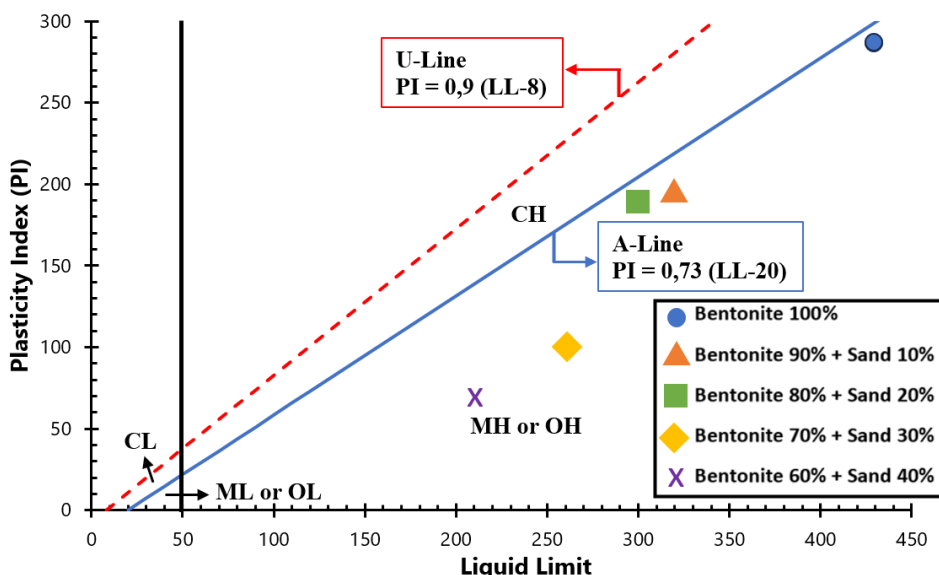


Figure 11. Casagrande plasticity chart with all specimens plotted (modified from Casagrande, 1932)

#### 4.2 Suspension Settling Model Results

The suspension settling model provides a relationship between settling time and slurry height, allowing for the determination of the critical height and time to estimate the boundary between suspension and viscous liquid states. The result (Figure 12) shows that the concentration controlled the settling rate; the higher the concentration, the faster the sediment settled.

Figure 13 illustrates the method for determining the critical time and height, using the tangent and sludge lines. Where the tangent line represents the slurry height and settling time curve, and the sludge line is a theoretical line that has a  $45^\circ$  angle that starts from zero. The compression point, or critical point, is the point of intersection of the tangent and sludge lines and can be used to determine  $v_c$  and  $H_c$ .

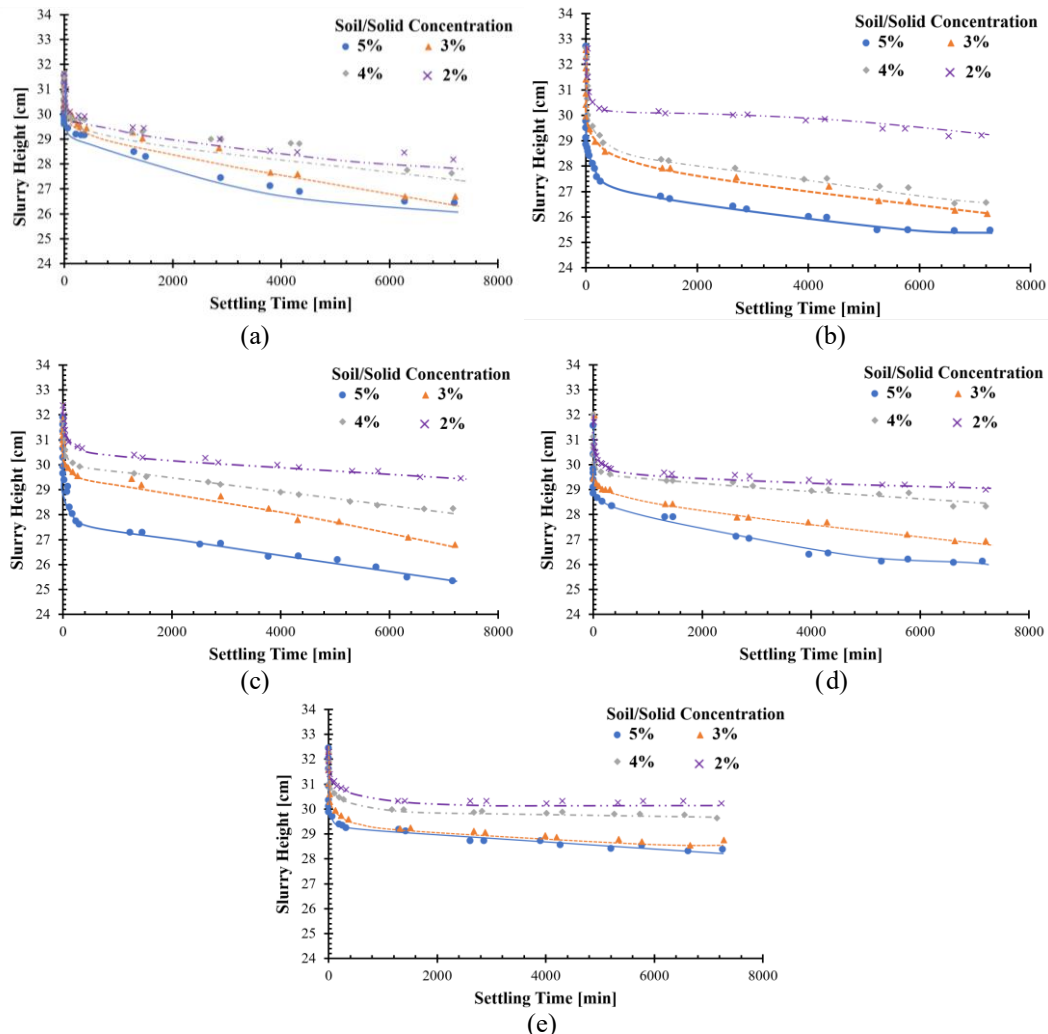


Figure 12. Suspension settling model observation result for each concentration and sample variation: (a) 100% Bentonite, (b) 90% Bentonite 10% Sand, (c) 80% Bentonite 20% Sand, (d) 70% Bentonite 30% Sand, and (e) 60% Bentonite 40% Sand

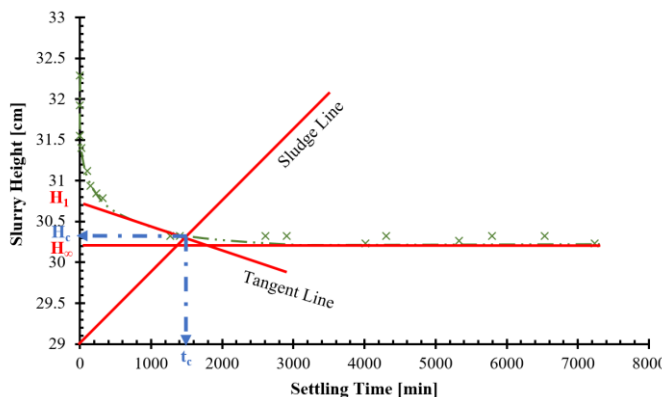


Figure 13. Illustration on how to define  $H_1$ ,  $H_\infty$ ,  $H_c$ , and  $t_c$  in suspension settling model for bentonite 60% sand 40% with 20 g concentration

Based on the method and data above, the  $H_0$ ,  $H_1$ ,  $H_c$  and  $t_c$  for all specimens with their respective concentration can be determined. Then, the critical settling rate ( $v_c$ ) can be calculated using equation 3. The results are tabulated in Table 2. The results show that sand and sample concentrations do not impact the  $v_c$  and  $H_c$  values, caused there are no clear trend about  $v_c$  and  $H_c$ . The results (Table 2) show that bentonite has a very slow settling rate ( $v_c$ ), so the smaller the  $v_c$ , the longer it takes to reach the critical condition.

Table 2. Critical sedimentation velocity for all specimens

Samples	Samples Concentration [g]	$H_0$ [cm]	$H_1$ [cm]	$H_c$ [cm]	$t_c$ [min]	$v_c$ [cm/s]
100% Bentonite	50	31.5	28.5	27.2	3300	$3.9 \times 10^{-4}$
	40	31.5	29.8	29.0	1440	$5.6 \times 10^{-4}$
	30	31.0	29.8	29.0	2300	$3.5 \times 10^{-4}$
	20	31.3	29.7	28.6	4500	$2.4 \times 10^{-4}$
90% Bentonite + 10 % Sand	50	32.5	28.8	27.8	2600	$3.8 \times 10^{-4}$
	40	32.2	28.1	27.8	2400	$1.3 \times 10^{-4}$
	30	31.5	28.0	27.4	3500	$1.7 \times 10^{-4}$
	20	32.0	30.0	29.6	3800	$1.1 \times 10^{-4}$
80% Bentonite + 20% Sand	50	31.8	27.8	25.9	4600	$4.1 \times 10^{-4}$
	40	31.7	29.5	28.0	4300	$3.5 \times 10^{-4}$
	30	31.6	29.5	28.5	5300	$1.9 \times 10^{-4}$
	20	32.3	30.5	30.2	3500	$9.0 \times 10^{-5}$
70% Bentonite + 30% Sand	50	31.5	28.0	27.0	3200	$3.1 \times 10^{-4}$
	40	31.0	28.8	27.9	4100	$2.2 \times 10^{-4}$
	30	32.0	29.2	29.0	5500	$4.0 \times 10^{-5}$
	20	31.7	31.1	29.55	1900	$8.2 \times 10^{-4}$
60% Bentonite + 40% Sand	50	32.2	29.1	28.75	5600	$6.0 \times 10^{-5}$
	40	31.7	29.0	28.7	4400	$7.0 \times 10^{-5}$
	30	32.3	30.3	29.9	2500	$1.6 \times 10^{-4}$
	20	32.3	30.8	30.3	1500	$3.0 \times 10^{-4}$

#### 4.3 Cylinder Test Results

The CST was conducted on the bentonite sediment to determine the  $c_u$  value and verify whether the sample had passed the critical condition. For the specimens prepared, the CST can be performed within an LI range of 1.4 to 2.9. Beyond LI 2.9, the cylinder sinks completely due to its weight exceeding the undrained shear strength ( $c_u$ ) and the buoyant force acting on its entire volume. Figure 14 shows an exponential decay relationship between LI and  $c_u$ , i.e. the  $c_u$  value reduces with increasing LI value. The increase in sand amount causes the  $c_u$  value to increase for the initial water content (low LI).

The cylinder diameter also influences the determination of  $c_u$  values. Figure 15 illustrates the influence of changing the cylinder diameter, which leads to a change in its weight and contact surface. The results show that the highest  $c_u$  value was obtained with a 50 mm cylinder diameter, and the smallest value was obtained with a 30 mm CST diameter. At the initial LI, the  $c_u$  value for each diameter shows quite significant gaps, but when the LI exceeds 2.4, the gaps become tighter.

#### 4.4 Estimating the Flow Limit Value

From the CST and suspension settling model, the value of FL was obtained. Where the  $c_u$  values are zero for CST. Figure 16 shows the CST result for the bentonite sediment after the suspension settling mode.

The CST shows the same FL value at LI equal to 6 for each diameter variation (Figure 15), and the bentonite mixed with sand obtained the same LI value for all sand variations in LI, water content (w) and ratio of FL over LL (Table 3). Table 4 shows the results for the bentonite sediment FL value using CST. According to the suspension settling model, the FL value can be determined from the water content from sediment samples. In this context, FL is considered the critical condition in the suspension model; the FL value is taken from the average of all variations of soil concentrations (Table 5).

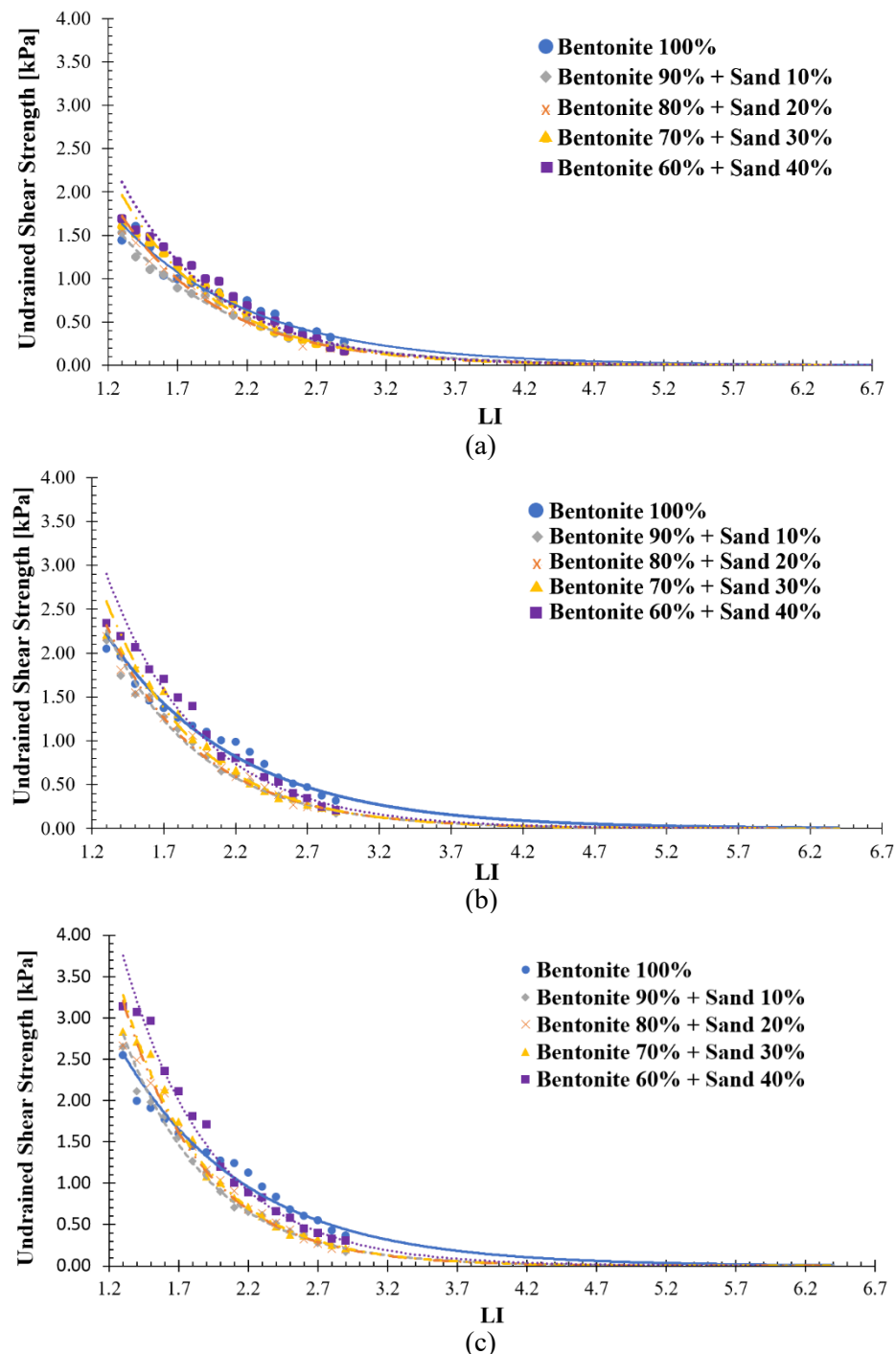


Figure 14. CST result for cylinder diameter (a) 30 mm, (b) 40 mm, and (c) 50 mm.

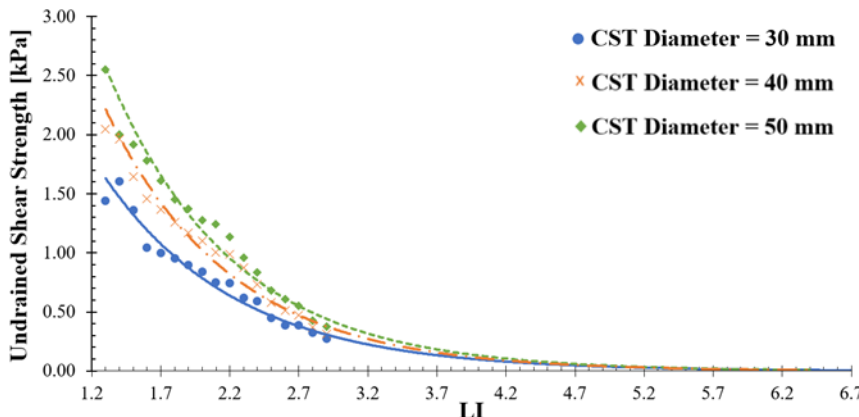


Figure 15. Comparison of CST results for 100% bentonite specimen tested with different cylinder diameters

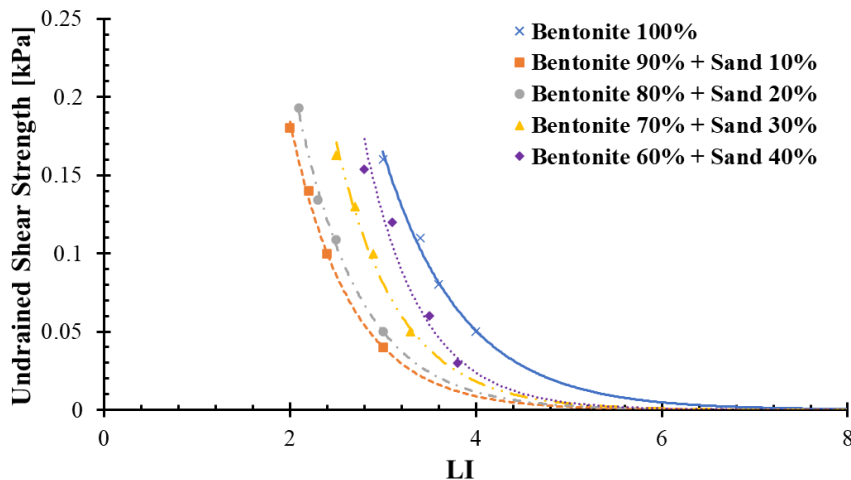


Figure 16. The CST results from the suspension settling samples

Table 3. Flow limit value from CST

Samples	FL	LI	FL/LL
Bentonite 100%	1840	6.0	4.28
Bentonite 90% + Sand 10%	1061	4.8	3.32
Bentonite 80% + Sand 20%	1022	4.8	3.41
Bentonite 70% + Sand 30%	868	4.8	3.33
Bentonite 60% + Sand 40%	742	4.8	3.53

Table 4. Flow limit value from CST after suspension settling model simulation

Samples	FL	LI	FL/LL
Bentonite 100%	2122	7.0	4.9
Bentonite 90% + Sand 10%	1295	6.0	4.0
Bentonite 80% + Sand 20%	1250	6.0	4.2
Bentonite 70% + Sand 30%	932	5.2	3.6
Bentonite 60% + Sand 40%	798	5.2	3.8

Tables 3 and 4 show that the sand materials contribute to reducing the FL value. Where the effect of adding sand to pure bentonite is quite significant, the value can drop by around 14 to 25%. However, the increase of sand concentration from 10% to 40% does not reduce the FL

According to Tables 3, 4, and 5, different approaches lead to different results. Based on all the tests using the suspension settling model, the smallest FL value is yielded, while the bentonite sediment CST FL value is the largest. Many factors can influence the results, including the CST and the CST after suspension settling model. One of them is the boundary effect, where in the small concentration samples, the resulting slight sediment can lead to the failure plane from the CST not being fully developed, which affects the  $c_u$  values. The other aspect where the CST from the suspension settling model is not tested until the cylinder entirely drowns; additionally, the results fall within a narrow range of  $c_u$  values, which can affect the trendlines.

Table 5. Flow limit value from suspension settling model simulation

Samples	FL	LI	FL/LL
Bentonite 100%	1135	3.5	2.6
Bentonite 90% + Sand 10%	593	2.4	1.9
Bentonite 80% + Sand 20%	585	2.5	2.0
Bentonite 70% + Sand 30%	564	2.9	2.2
Bentonite 60% + Sand 40%	532	3.3	2.5

The differences in the results of these three tests are due to the different approaches that use different principles. Each test has advantages and disadvantages. For example, CST can determine the magnitude of the  $c_u$  value to a relatively small value but has difficulty in estimating when the  $c_u$  value will reach zero. As for the suspension settling model, the main difficulty in determining the FL value lies in its relative subjectivity when determining the critical suspension settling time. Although the suspension settling model has its shortcomings when compared to CST, this model can at least provide an overview of the sedimentation process of soil suspension towards viscous liquid.

The FL/LL ratio obtained from this set of experiments ranged from 1.9 to 2.6. When the results were compared to those of the previous study by Park and Nong (2013), the FL/LL ratio ranged from 1.5 to 2.21, which is close enough to the results of the suspension settling model. A previous study by Widjaja and Florentini (2020) and Shen and Tsai (2024) reported an FL/LL ratio of around 1.5 to 2, which differs significantly from the results of this study.

The gap between this study's results and previous studies may be attributed to the differences in bentonite mineralogy (manufacturer) (Chen, 1975). Chen (1975) states that mineralogy can be estimated using the liquid limit (LL) and plasticity index (PI). In this case,  $\text{Na}^+$  bentonite was used, as Park and Nong (2013) indicated the use of  $\text{Ca}^{++}$  bentonite, and Widjaja and Florentini (2020) indicated the use of  $\text{Mg}^{++}$  bentonite from the typical LL and PI value ranges (based on the typical LL and PI value that Chen (1975) stated). According to Widjaja *et al.* (2024), the CST can determine the  $c_u$  value to a much greater extent than the LI in other tests. Another aspect of the significant difference in the FL value is the regression; Park and Nong (2013) determined the regression by using a sharp angle to determine when the  $c_u$  hits zero, which can be subjective and lead to inconsistent results. In this study, a regression was performed to make the regression smoother, thereby obtaining more objective and consistent results. The CST shows more consistent results for all conditions, as opposed to the suspension settling model, due to the latter having a higher degree of disturbance in water content determination, and the settling phase having already passed through the critical condition.

## 5 CONCLUSIONS

This study employed the CST as well as the suspension settling model to determine the flow limit (FL) values for bentonite and bentonite plus sand mixtures. Three diameter variations were used for CST, and five concentrations of samples were used in the suspension settling model. CST determines the FL from the viscous liquid state using  $c_u$  values. In contrast, the settling model determines it from the suspension state based on the critical condition when it starts behaving like a viscous liquid.

The results show that the suspension settling model yielded the smallest FL results for all variations, while CST for the bentonite sediment was the largest. The CST results show consistent FL/LL for the three cylinder diameters used. In the suspension settling model, the effect of sand concentration in the samples has no clear patterns that can be drawn. However, for low LI value, there is observable trend for the sand's effect on the  $c_u$ , with the value increasing with increasing sand concentration. This makes the trendline steeper and causes the FL value to be consistent for all samples that were mixed with sand. Although FL value obtained from the two approaches are not the same, this study provides an overview on how FL values can be obtained from different approaches.

The results of this study show higher FL values than those of previous studies, particularly in the CST results. This can occur due to the varying mineral composition of the bentonite samples, differences in test apparatus capacity, and varying approaches to estimating the FL value. Further studies should consider evaluating other soil types, especially natural soils, and utilize alternative apparatus to determine the FL value, such as the laboratory vane shear test. For the CST, a sensitivity analysis for dimensions, especially length and weight variations, needs to be done. Another factor that needs to be considered is the soil's mineralogy, and proposes a new method that is more objective, which may help explain the results gaps for each soil sample.

## DISCLAIMER

The authors declare no conflict of interest.

## AVAILABILITY OF DATA AND MATERIALS

All data are available from the author.

## ACKNOWLEDGMENTS

The authors acknowledge Parahyangan Catholic University for the opportunity to conduct this research.

## REFERENCES

Atterberg, A., 1911. Über die physikalische Bodenuntersuchung und über die Plastizität der Tone. *Internationale Mitteilungen für Bodenkunde*, 1, pp. 10-43.

Bain, D. C. 2009. Bentonites Versatile Clays. *Elements*, 5(2), pp. 83-116.

Casagrande, A., 1932. Research on the Atterberg Limits of Soil. *Public Roads*, 13(8), pp.121-136.

Chen, F. H., 1975. *Foundations on Expansive Soils*. Elsevier Scientific Publishing Company.

Conca, F., 2014. *Solid–Liquid Separation in the Mining Industry*. Cham: Springer Switzerland. <https://doi.org/10.1007/978-3-319-02484-4>

Coe, H.S., & Clevenger, G. H., 1916. *Methods for Determining the Capacity of Slime Settling Tanks*. *Transactions American Institute of Mining Engineering (AIME)*, 55, pp. 356-385.

Egolf, C. B., & McCabe, W. L., 1937. *Rate of sedimentation of flocculated particles*. *Transactions AIChE*, 33, pp. 620-642.

El-Shall, H., Bogan, M., & Moudgil, B., 1993. Mathematical Modelling of Settling of Solid Suspensions. *Mining, Metallurgy and Exploration*, 10, pp. 57–61. <https://doi.org/10.1007/BF03403000>

Gary, M., McAfee, R. J., Wolf, C. L., 1973. *Glossary of Geology*. American Geosciences Institute (AGI).

Germaine, J. T., & Germaine, A.V., 2009. *Geotechnical Laboratory Measurements for Engineers*. New Jersey: Mc. Wiley & Sons, Inc.

Kynch, G. J., 1952. A Theory of Sedimentation. *Transactions of the Faraday Society*, 48, pp. 166-176.

Mishler, R. T., 1912. Settling Slimes at the Tigre Mill. *Engineering Mining Journal*, 94(14), pp. 643-646.

O'Brien, J. S., 2003. Reasonable Assumption in Routing a Dam Break Mudflow. *3rd Conference on Mud and Debris Flows on Proceedings of Debris Flow Hazards Mitigation*.

Park, S., & Nong, Z., 2013. *A Proposal of Flow Limit for Soils at Zero Undrained Shear Strength*. *Journal of the Korean Geotechnical Society*, 29 (1), pp. 73-84. <https://doi.org/10.7843/kgs.2013.29.11.73>

Shen, M., & Tsai, Y., 2024. Application of Cohesive Soil Flow Limit and Slope Critical Flow Angle. *Geotechnical Research*, 11 (2), pp. 88-99. <https://doi.org/10.1680/jgere.23.00035>

Vallejo, L. E., & Scovazzo, V. A., 2003. Determination of the Shear Strength Parameters Associated with Mudflow. *Soils and Foundations*, 43 (2), pp. 129-133. [https://doi.org/10.3208/sandf.43.2\\_129](https://doi.org/10.3208/sandf.43.2_129)

Vallejo, L. E., 2019. The Measurement of the Undrained Shear Strength of Muds Using a Cylinder. *Cancun, Geotechnical Engineering in the XXI Century: Lessons learned and future challenges*, pp. 409-415.

Wesley, L. D., 2009. *Fundamentals of Soil Mechanics for Sedimentary and Residual Soils*. John Wiley & Sons, Inc.

Widjaja, B., & Florentini, F., 2020. Determining Flow Limit Using Fall Cone Penetrometer Test. *Jakarta, The 24<sup>th</sup> Annual National Conference on Geotechnical Engineering*.

Widjaja, B., Pratama, I. T., Hartono, I., & Limowa, B., 2024. Laboratory Study on Vallejo and Scovazzo's Methods in Estimating the Rheology Parameters of Bentonite and Kaolinite Muds. *Civil Engineering Dimension*, 26 (2), 51- 62. <https://doi.org/10.9744/ced.26.1.51-62>

Zhang, L., Yang, K., Liu, F., Zhu, L., Xia, W., Wang, H., He, X., & Hou, Y, 2025. An Approach to Determine Settling Properties of Flocculated Tailings Suspensions Based on a Single Batch Settling Test. *Particuology*, 102, pp. 15-26. <https://doi.org/10.1016/j.partic.2025.04.003>